ISSN 1023-1935, Russian Journal of Electrochemistry, 2014, Vol. 50, No. 8, pp. 756–772. © Pleiades Publishing, Ltd., 2014.
Original Russian Text © G.R. Nasybullina, V.V. Yanilkin, A.Yu. Ziganshina, V.I. Morozov, E.D. Sultanova, D.E. Korshin, V.A. Milyukov, R.P. Shekurov, A.I. Konovalov, 2014, published in Elektrokhimiya, 2014, Vol. 50, No. 8, pp. 841–857.

Electrochemical Control of Association and Deposition of Tetraviologen Calix[4]resorcin

G. R. Nasybullina, V. V. Yanilkin[z], A. Yu. Ziganshina, V. I. Morozov, E. D. Sultanova, D. E. Korshin, V. A. Milyukov, R. P. Shekurov, and A. I. Konovalov

Arbuzov Institute of Organic and Physical Chemistry, Russian Academy of Sciences, Kazan Scientific Center, Kazan, Russia

Received March 20, 2013

Abstract—The association and deposition of tetraviologen calix[4]resorcin MVCA-C_5^{8+} can be controlled using the electrochemical reduction–reoxidation cycle of viologen units. The monomeric MVCA-C_5^{8+} was converted into the highly molecular $(MVCA\text{-}C_5^{4+\bullet})_n$, associate (π-polymer) by reducing it to the MVCA-$C_5^{4+\bullet}$ tetra(radical cation) and completely returns to the starting monomeric state by reverse oxidation. The reduction to the neutral state MVCA-C_5^0 allowed calixresorcin to pass from solution to precipitate and the reverse oxidation led to its returning in solution.

Keywords: calix[4]resorcin, methylviologen, association, precipitation, electrochemical control

DOI: 10.1134/S1023193514080096

INTRODUCTION

N,N'-disubstituted bipyridinium dications (viologens) are among the most important organic electron-accepting structural elements that have recently attracted considerable attention due to their redox properties. Since the mid-20th century, it was known [1] that they are reversibly reduced in close ranges of potentials by a two-stage process that forms the stable radical cation $V^{\bullet+}$ and diamine V^0, respectively (Scheme 1). The properties of viologens change from strong electron acceptor to strong electron donor during the reduction. The compounds also change in color from colorless to blue and yellow, respectively [1].

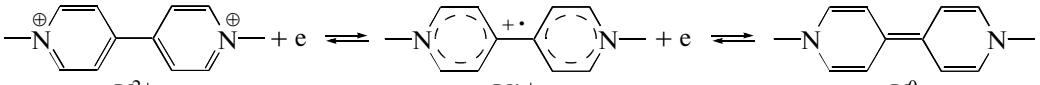

Scheme 1. Reversible two-stage reduction of MV^{2+}.

Increased interest in viologens in recent years was explained by the fact that viologen units react with electron-donating compounds to form donor-acceptor complexes [2–39], which dissociate after the partial or complete reduction of viologen. This underlies the functioning of supramolecular systems with electroswitchable and electrochemically controlled properties [35–39] and molecular devices and machines with a catenane [2–26], rotaxane [2, 24–32], and pseudorotaxane structure [13, 31, 33, 34].

An interesting property of viologens is the liability of their radical cations to undergo π-dimerization [40], i.e., the interaction of the π-systems of two radicals with electron coupling but without forming a σ-bond [41]. π-Dimerization depends strongly on the medium [42, 43], temperature [44], concentration [44], and the structure of the radical cation [45–47]. The UV spectra clearly show π-dimerization as an additional wide absorption band in the long-wave region (~850–950 nm), which appears at increased concentrations of the radical cation [48]. π-Dimerization of radical cations leads to a change in the color of the solutions of radical cations from blue to violet [48]. The π-dimerization effect was used to create molecular devices [49–52].

[z] Corresponding author: yanilkin@iopc.ru (V.V. Yanilkin).

To create supramolecular systems with electrochemically controlled properties, we previously studied the binding of calix[4]resorcin tetrasulfonate [35], the complex $[Fe(CN)_6]^{4-}$ tetraanion [36], and the dianion of amphiphilic 1,5-bis(*para*-sulfonatophenyl)-3,7-diphenyl-1,5-diaza-3,7-diphosphacyclooctane with amphiphilic tetramethylviologen calix[4]resorcin octacations that differ in the length of the hydrocarbon radical in the resorcinol fragments (MVCA-C_n^{8+}, where n = 1, 5) in solvents with different water and dimethylsulfoxide (DMSO) contents and $NaClO_4$ or NaCl supporting solutions [37, 39]. MVCA-C_n^{8+} is reduced in two stages in all solvents. The first stage involves the transition of four electrons to four viologen units, forming the MVCA-$C_n^{4+\bullet}$ tetra(radical cation), which further undergoes four-electron reduction to the neutral compound MVCA-C_n^0 at the second stage (Scheme 2). The transfer of four electrons occurs at the same potential at each stage. Supramolecular systems with electrochemically controlled binding (MVCA-C_5^{8+}) and aggregation (MVCA-C_1^{8+}) were created on the basis of the redox transformations of viologen units.

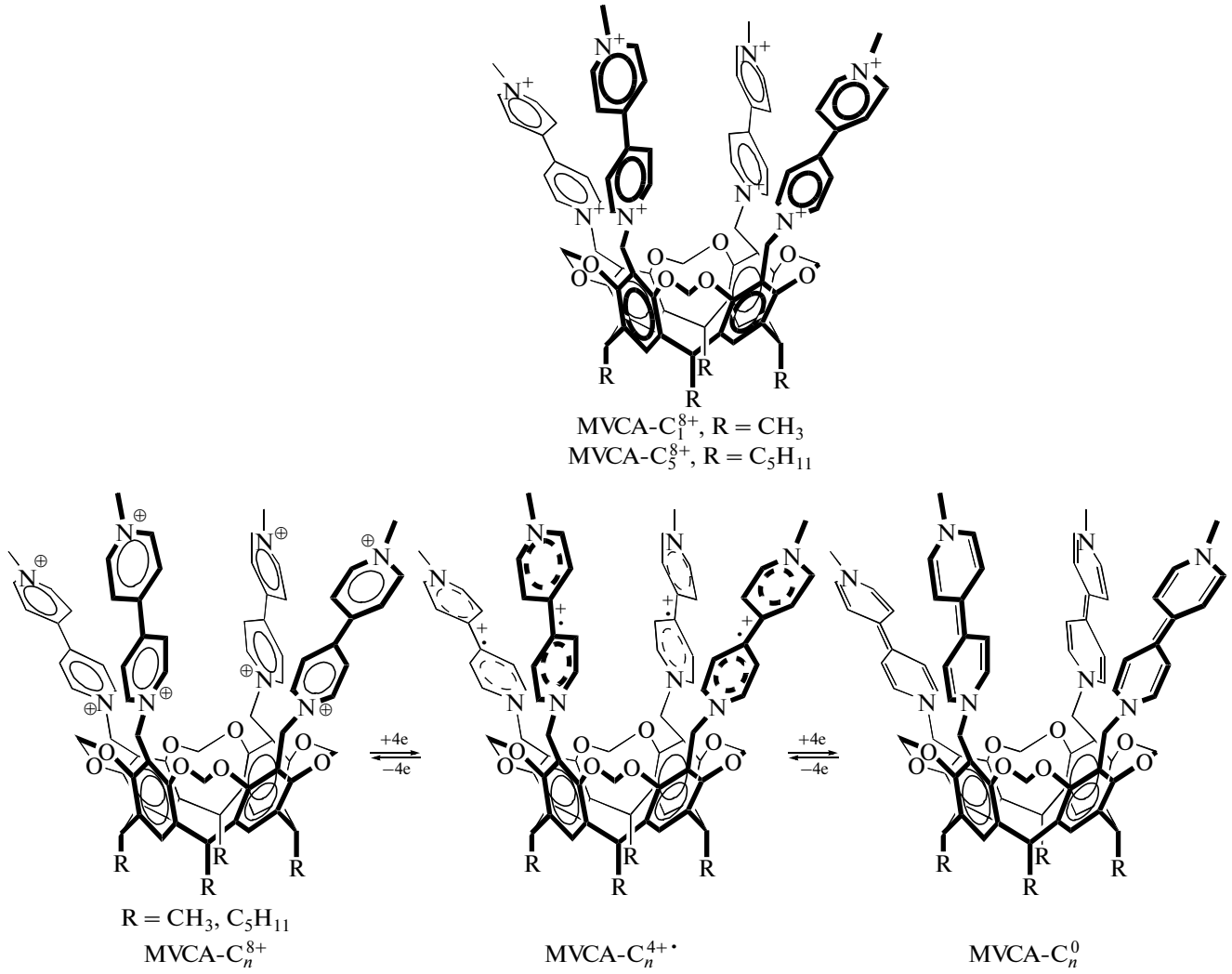

Scheme 2. Reversible two-stage reduction of MVCA-C_n^{8+} (n = 1, 5).

During the reduction of MVCA-C_n^{8+} at controlled potentials of the first stage under the conditions of large-scale electrolysis in these systems, the solution becomes violet, which points to π-dimerization of the radical cations of viologen fragments. Since there are four viologen units on the calixresorcin platform, both intra- and intermolecular dimerizations are possible in the tetra(radical cation). In contrast to the examples from the literature [40–52], the latter process in this case can lead to the formation of not only π-dimers, but also π-oligomers (π-polymers). Their formation opens up prospects for creating a system with an elec-

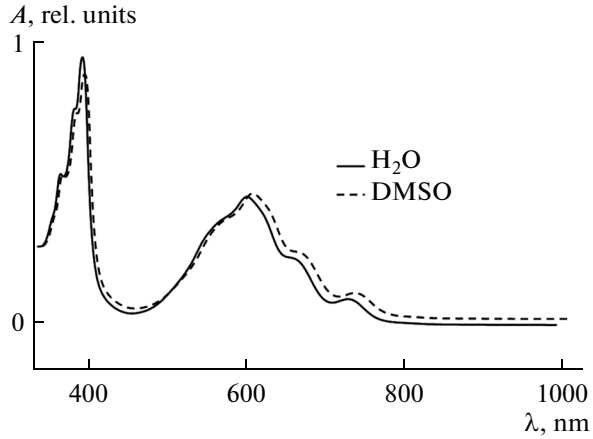

Fig. 1. Normalized UV spectra of methylviologen in water and DMSO ($C = 0.1$ mM) after the reduction with metallic zinc.

trochemically controlled state in the form of a monomer or oligomer from tetraviologen calix[4]resorcins by simply switching the potential from the steady state to the first-stage reduction potential and back. In this connection and from the viewpoint of more profound rationalization of previously obtained data, we investigated in detail the stepwise reduction of MVCA-C_5^{8+} in aqueous organic (dimethylformamide (DMF), DMSO) solvents with various contents of the organic component, paying major attention to π-dimerization. This communication presents the results of this study.

EXPERIMENTAL

The studies were performed by cyclic voltammetry (CV), electrolysis, and UV and EPR spectroscopy.

The cyclic voltammograms were recorded using a PI-50-1 potentiostat on an H 307/2 XY recorder (without *IR* compensation) in an inert atmosphere (nitrogen). The working electrode was a glassy carbon (GC) disc electrode ($\partial = 3.4$ mm) pressed into Teflon (fluoroplast). The electrode was cleaned by mechanically polishing it before each measurement. Platinum wire was an auxiliary electrode. The potentials were measured and are given relative to the saturated calomel electrode (s.c.e.) having a potential of –0.41 V relative to the formal potential of the Fc/Fc^+ redox system. The temperature was 295 K. The diffusion character of the peak currents i_p was proven using the theoretical form of the voltammogram and the linear dependence $i_p - v^{1/2}$, the adsorption nature was confirmed by the presence of an adsorption maximum and the linear $i_p - v$ dependence (the potential scan rate v was varied from 10 to 200 mV/s) [53].

The electrolysis was performed in a three-electrode glass diaphragm (porous glass) cell in a potentiostatic mode in an atmosphere of an inert gas (nitrogen) using a PI-50-1 potentiostat. During the electrolysis, the solution was stirred with a magnetic stirrer. The working electrode was glassy carbon tissue ($S = 18$ cm^2), the auxiliary electrode was platinum wire, and the reference electrode was s.c.e. The solutions were monitored by CV on the indicator glassy carbon disc electrode ($\partial = 3.4$ mm) directly in the electrolyzer during the electrolysis.

For electrolysis of the MVCA-C_5^{8+} system, the working solution with a volume of 20 mL was prepared by dissolving MVCA-$C_5^{8+} \cdot 8Cl^-$ ($C = 0.5$ mM) (18.4 mg) and the $NaClO_4$ supporting salt (245 mg) or NaCl ($C = 0.1$ M) (117 mg) in 90% aqueous DMF or 30% aqueous DMSO (30 vol % DMSO). For electrolysis of the MVCA-C_5^{8+}–ferrocene (Fc) system, Fc ($C = 0.5$ mM) (1.9 mg) was added to the above-mentioned solution; for the MVCA-C_5^{8+}–ferrocenyl(H-phosphine) acid system, an acid (2.5 mg) was added. A supporting electrolyte solution was poured into the auxiliary space. The electrolysis was conducted at controlled potentials of the first (from –0.6 to –0.8 V) and second (from –1.1 to –1.4 V) reduction peaks and at the potential of reoxidation to the dication state (from +0.4 to +0.5 V) until the current became constant.

A spectrophotometric study was performed on a Perkin Elmer Lambda-35 spectrophotometer using 10 mm quartz cells at 295 K. The EPR spectra were recorded on a SE/X 2544 Radiopan spectrometer (Poland) and simulated using the "Winsim v.1.0, 2002" program. The results were processed with the Microcal Origin program.

MVCA-$C_5^{8+} \cdot 8Cl^-$ was synthesized by the procedure of [35]. Ferrocenyl(H-phosphine) acid (Fc-P(O)(H)OH) was prepared by the procedure of [54]. The commercial reagents were the salts $MV^{2+} \cdot 2Cl^-$, NaCl, $NaClO_4$, and Fc. The DMF solvent (Panreac) was used without further purification. All the salts dissociate well in the chosen solvents; therefore, here we mainly operate on ions unless stated otherwise. DMSO was purified by the procedure of [55]; twice distilled water was used.

RESULTS AND DISCUSSION

Spectrophotometric Studies

The π-dimerization of radical cations is readily proven by UV spectroscopy; therefore, the MVCA-$C_5^{4+\bullet}$ radical cations were mainly studied by this method. The absorption spectra were recorded for 0.02 or 0.04 mM aqueous organic solutions of MVCA-C_5^{8+} reduced with metallic zinc. The organic component (DMF, DMSO) was varied over a wide range (every 10%) from 0 to 100 vol %. For comparison, the UV spectrum of the methylviologen MV^{2+} radical cation (0.1 mM) was recorded. For MV^{2+}, the spectrum of the monomeric $MV^{+\bullet}$ radical cation was recorded in all solvents; the π-dimers were not found at the low concentration used (Fig. 1). For MVCA-C_5^{8+}, the monomer–π-dimer ratio depends on the medium. In 100% organic solvents, the solution contained only the

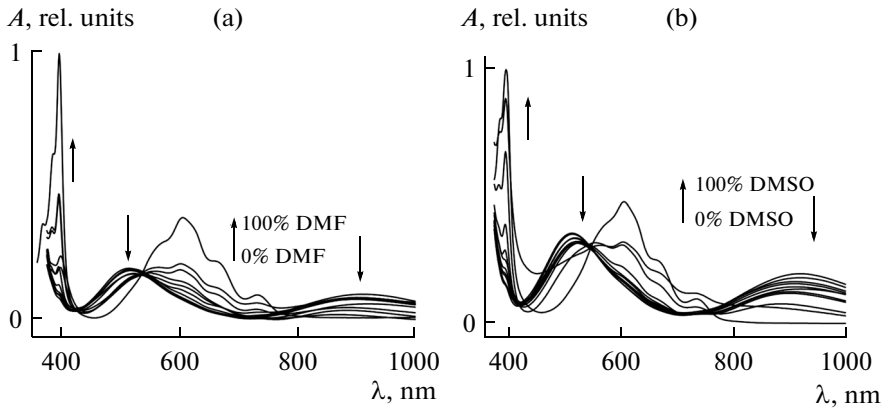

Fig. 2. Normalized UV spectra of MVCA-$C_5^{4+\bullet}$ at different (a) water/DMF and (b) water/DMSO ratios after the reduction with metallic zinc. C = (a) 0.02 mM and (b) 0.04 mM.

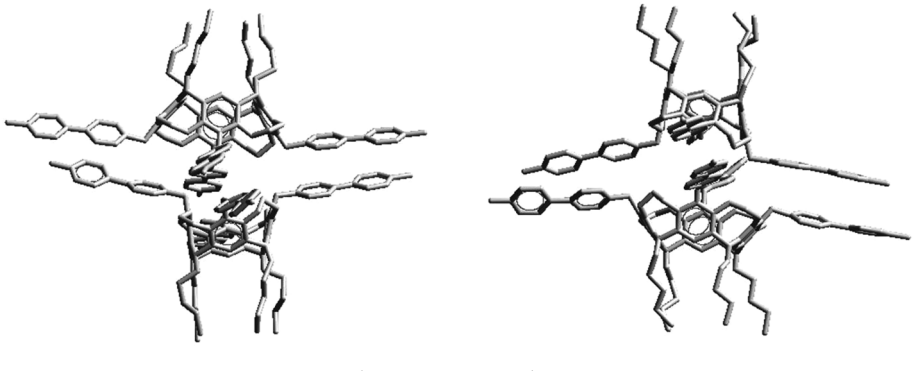

Fig. 3. Structure of the π-dimer of the MVCA-$C_5^{4+\bullet}$ tetra(radical cation) with four-center interaction modeled with MM+ (HyperChem 8.0).

monomer radical cations of viologen units (Figs. 2a, 2b). The addition of 10% water in the solution already led to the formation of π-dimers, as indicated by the transformation of the whole spectrum and especially the appearance of a wide absorption band at ~900 nm. As the water content increased, the monomer radical cation fraction decreased and the π-dimer fraction simultaneously increased. In 100% water, the monomer was present in minor quantities; the main part of the viologen radical cations MVCA-$C_5^{4+\bullet}$ was in the form of π-dimers. MM+ modeling of the tetra(radical cation) shows that intramolecular π-dimerization is impossible because of steric hindrances. At the same time, there are no pronounced limitations on intermolecular π-dimerization both for one- and two-center interactions and for three- and four-center ones (four radical cations of one molecule with four radical cations of another, Fig. 3). Consequently, the MVCA-$C_5^{4+\bullet}$ π-dimers in this case are the products of intermolecular π-dimerization. Note that these results were obtained for the concentration 0.02 (0.04) mM. Evidently, for more concentrated solutions (0.5 mM) used in the electrochemical experiment, the fraction of π-dimers will be much higher in all solvents irrespective of the number of interaction centers.

Electrochemical Studies

H_2O–DMF (90 vol % DMF)/0.1 M $NaClO_4$ medium. As in all previously studied organic and aqueous organic solvents [35–39, 56, 57], in this medium MVCA-C_5^{8+} (C = 0.5 mM) was also reduced stepwise (Fig. 4*a*), forming the stable MVCA-$C_5^{4+\bullet}$ tetra(radical cation) and the MVCA-C_5^0 neutral compound according to Scheme 1. The first reduction peak is a pure diffusion peak ($i \sim v^{1/2}$); the second peak and both reoxidation peaks also contain a small adsorption component. As a result, the second reduction peak is slightly more acute and higher than the first one and the potential difference between the first reduction and reoxidation peaks at low potential scan rates is lower than the theoretical value for single-electron reversible

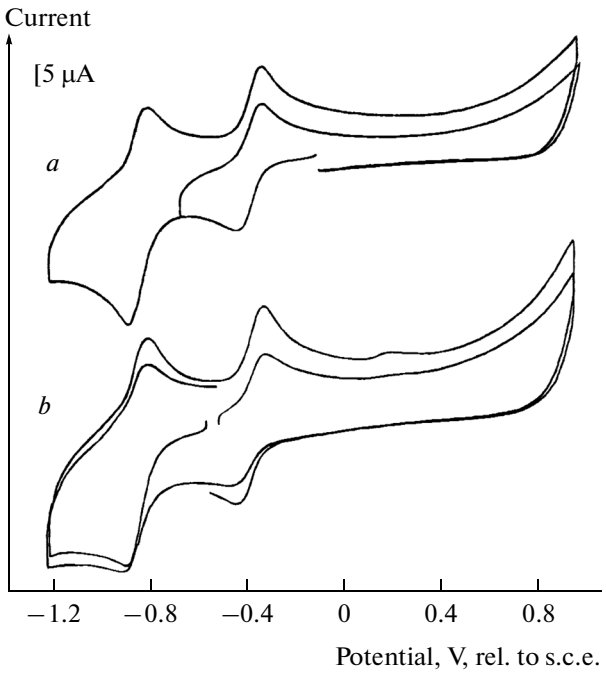

Fig. 4. CV curves of MVCA-C_5^{8+} (0.5 mM) in DMF–H_2O (90 vol % DMF)/0.1 M $NaClO_4$: (*a*) the starting solution and (*b*) the solution after the reduction at $E = -0.7$ V for 20 min. $v = 100$ mV/s.

processes (59 mV at 25°C [53]). Thus, at $v = 10$ mV/s, this difference is 40 mV. The potential of the first reoxidation peak is independent of the potential scan rate in the range 10–200 mV/s, and the reduction peak potential shifted toward negative values at increased v. The latter is the result of the subsequent π-dimerization reaction. When the working electrode was preliminarily maintained at the potential of generation of the radical cation form ($E = -0.6$ V) for 1 or 2 min and the CV was recorded at this potential, there were no significant changes on the CV curve. It follows from the set of obtained data that the radical cations are π-dimerized during the electrochemical reduction of MVCA-C_5^{8+} to MVCA-$C_5^{4+\bullet}$. The products of the reduction of calixresorcin are adsorbed on the electrode surface insignificantly. The low peak current of MVCA-C_5^{8+} is unusual in this system. The four-electron diffusion peak of its reduction equals the one-electron diffusion peak of ferrocene oxidation, which suggests the low diffusion rate of the MVCA-C_5^{8+} octacation compared with that of uncharged ferrocene (the diffusion coefficient is ~16 times lower).

The solution of MVCA-C_5^{8+} ($C = 0.5$ mM), which is slightly yellow in the initial state, starts to be colored blue immediately after large-scale electrolysis on a glassy carbon fabric at the potentials of the generation of the tetra(radical cation) ($E = -0.7$ V). In 2 min, the blue color becomes deep and changes to violet. This color persists during the whole electrolysis for 20 min ($Q \approx 6$ F/mol MVCA-C_5^{8+}) and during further recording of CV curves. After the electrolysis, the steady-state potential of the GC indicator electrode ($E_{st} = -0.55$ V) became higher negative than the potential of the first reduction peak of MVCA-C_5^{8+} ($E^1_{p,red} = -0.42$ V). This points to the practically quantitative reduction of MVCA-C_5^{8+} to MVCA-$C_5^{4+\bullet}$ and the absence of the starting MVCA-C_5^{8+} and other possible intermediates of the partial reduction of the first stage of MVCA-$C_5^{m+1\bullet}$ (MVCA-$C_5^{7+1\bullet}$, MVCA-$C_5^{6+2\bullet}$, and MVCA-$C_5^{5+3\bullet}$). The CV curve of the electrolysate recorded with the initial potential scan from the steady-state potential toward the anode values shows one oxidation peak of MVCA-$C_5^{4+\bullet}$, whose potential exactly equals the potential of the first peak of reoxidation on the CV curve of MVCA-C_5^{8+} (Fig. 4*b*). The height of this peak is 15% lower than that of the first peak of the reduction of MVCA-C_5^{8+} in the starting solution. The reverse branch of the curve contains the peaks of re-reduction of MVCA-C_5^{8+} to MVCA-$C_5^{4+\bullet}$ and the reduction of MVCA-$C_5^{4+\bullet}$ to MVCA-C_5^0. The picture was similar when CV was recorded with the initial potential scan toward the cathode values.

The violet color of the solution suggests π-dimerization of the MVCA-$C_5^{4+\bullet}$ radical cations of viologen units. The intermolecular π-dimerization is indicated not only by the calculated data, but also by the change in the color of solution from blue to violet in the course of electrolysis. At the start of electrolysis, i.e., at low tetra(radical cation) concentrations, the (blue) color of the solution corresponds to the monomer radical cations of the viologen units. At higher electrolysis times and hence higher tetra(radical cation) concentrations, the (violet) color of the solution corresponds to the π-dimers.

The π-dimers should be reduced and oxidized less readily than the monomers. The absence of additional signals of both the starting compound MVCA-C_5^{8+} and MVCA-$C_5^{4+\bullet}$ on the CV curve is due to the high rate of π-dimerization and dissociation of the π-dimers. π-Dimerization leads to an increase in the molecular mass of the species and accordingly to a decrease in the diffusion coefficient, which just shows itself as decreased oxidation currents of MVCA-$C_5^{4+\bullet}$ compared with the reduction currents of MVCA-C_5^{8+}.

During the reverse oxidation of the solution at $E = +0.4$ V, the violet color of the solution which it acquired during the reduction in the preceding electrolysis changes to blue in 3 min. The color gradually becomes less deep with time and after 14 min of electrolysis, the solution corresponds, in its yellowish

color and CV curves, to the starting solution of MVCA-C_5^{8+} (Fig. 4*a*).

The repeated reduction–reoxidation cycle leads to the same results. Thus, we performed double electrochemical switching of MVCA-C_5^{8+} to a mixture of the monomer and π-dimer tetra(radical cation) and back with reversible switching of the color of the solution: pale yellow ⇔ blue ⇔ violet.

The neutral form MVCA-C_5^0 was also generated at $E = -1.2$ V. The electrolysis was performed for 36 min until the currents became constant. The blue color appeared immediately; after 1.5 min, the solution became violet and in 11 min, it acquired brownish red coloring, which became deeper with time and remained to the end of electrolysis. The steady-state potential of the GC electrode ($E_{st} = -0.84$ V) corresponds to the second reduction peak of MVCA-C_5^{8+}. The solution actually contained the neutral form. On the CV curve of the electrolysate, the oxidation stages are lowered. After reverse oxidation at $E = +0.4$ V (18 min), the color of the solution became at first violet and blue and then yellow. The CV curve of this state of the system corresponds to the starting solution; i.e., after the cycle of reduction of MVCA-C_5^{8+} to MVCA-C_5^0 at the potentials of the second stage and reverse oxidation, it completely returns to the starting MVCA-C_5^{8+} state. The obtained result indicates that MVCA-C_5^0 is stable for a long time.

As mentioned above, the diffusion coefficient of MVCA-C_5^{8+} is unusually low and still lower for the π-dimeric tetra(radical cation), which followed from the CV curves of MVCA-C_5^{8+} and MVCA-$C_5^{4+\bullet}$. To confirm these conclusions additionally, we studied the reduction and reoxidation of MVCA-C_5^{8+} in the presence of equimolar amounts of ferrocene.

The starting solution was bright yellow. The CV curve contains the peaks of the reduction and reoxidation of MVCA-C_5^{8+} in the cathode region and the reversible peak of oxidation of Fc to Fc^+ at $E_p = +0.46$ V in the anode region (Fig. 5). The potentials and heights of all peaks correspond to the oxidation or reduction of free nonbonded particles.

During the generation of MVCA-$C_5^{4\bullet+}$ radical cations in the course of electrolysis at $E = -0.6$ V, the color of the solution changed in the same way as in the electrolysis in the absence of Fc. The blue coloring became pronounced at the start and then changed to violet after 4 min. The electrolysis was conducted for 33 min until the currents became constant.

According to the steady-state potential of the working electrode ($E_{st} = -0.40$ V), MVCA-C_5^{8+} was reduced to MVCA-$C_5^{4\bullet+}$ nonquantitatively in this case.

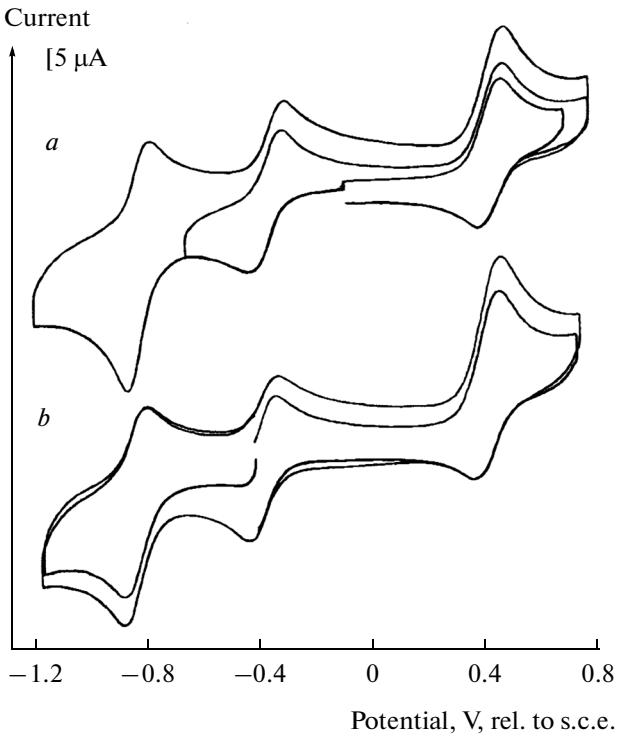

Fig. 5. CV curves of MVCA-C_5^{8+} (0.5 mM) + Fc (0.5 mM) in DMF–H_2O (90 vol % DMF)/0.1 M $NaClO_4$: (*a*) the starting solution and (*b*) the solution after the reduction at $E = -0.8$ V. $v = 100$ mV/s.

The CV curves of the electrolysate contain the oxidation peak of MVCA-$C_5^{4\bullet+}$ and the peak of oxidation of Fc to Fc^+ at a potential of +0.45 V, whose height increased 1.4-fold compared with that of the starting solution (Fig. 5). The reverse Fc^+ reduction peak corresponds, in its height and potential, to the peak for the starting solution. In this case, Fc really performs the function of a mediator; i.e., at Fc oxidation potentials, the monomer and π-dimer forms of MVCA-$C_5^{4\bullet+}$ are oxidized with Fc^+ generated electrochemically. The oxidation of the less mobile monomer and π-dimer forms of MVCA-$C_5^{4\bullet+}$ is accelerated due to the much higher mobility of Fc and Fc^+, which is reflected in the increase in the Fc oxidation peak current.

To return the system to its starting state, we oxidized it at the potential of oxidation of Fc to Fc^+ ($E = +0.4$ V). The similar oxidation in the system without ferrocene took 14 min, while in this case, the mediator oxidation took only 3.5 min. Already after 1.5 min, the violet solution became blue and after 2 min, the blue color vanished and the solution acquired its initial yellow coloring. The CV curve of this solution corresponds to that of the starting solution. The height of the Fc oxidation peak lowered to the initial value.

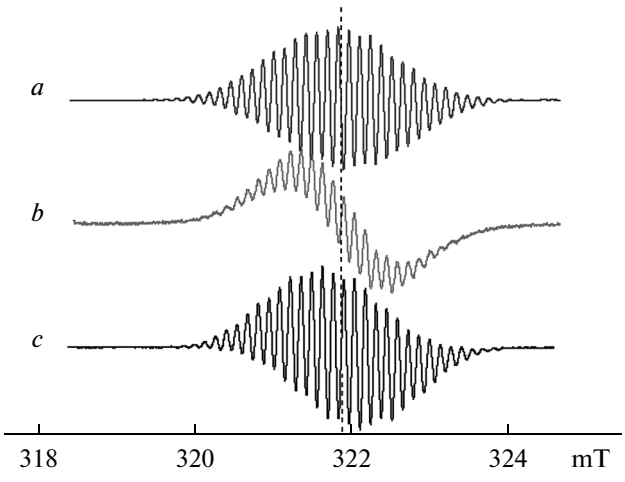

Fig. 6. EPR spectra of (*a*) dimethylviologen radical cations, (*b*) methylviologen fragment MVCA-$C_5^{4+\bullet}$, and (*c*) methylcetylviologen generated during the electrochemical reduction at the potentials of the first peaks of the reduction of dimethylviologen, methylcetylviologen, and MVCA-C_5^{8+} on a Pt electrode in 90% aqueous DMF/0.1 M $NaClO_4$.

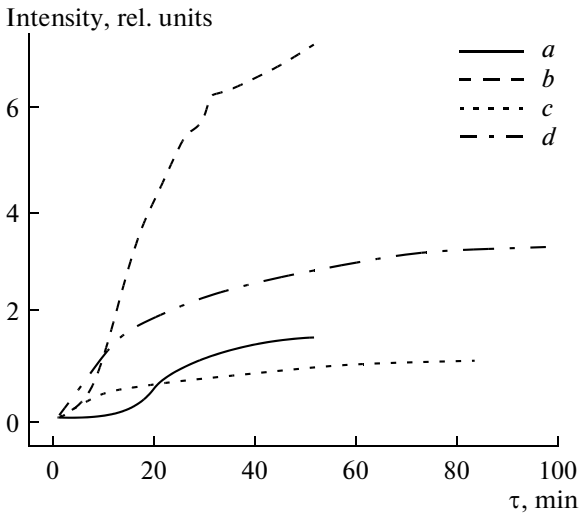

Fig. 7. Dependence of the signal intensity of radical species obtained by EPR in DMF–H_2O (90 vol % DMF)/0.1 M $NaClO_4$ for (*a*) $MV^{+\bullet}$ (C = 0.5 mM), (*b*) $MV^{+\bullet}$ (C = 2 mM), MVCA-$C_5^{4+\bullet}$, (*c*) (C = 0.125 mM), and (*d*) MVCA-$C_5^{4+\bullet}$ (C = 0.5 mM).

The cycle of electrolyses was repeated. The reduction was conducted at $E = -0.8$ V, which accelerated the process. The reduction lasted 14 min; the reverse oxidation also occurred within 3.5 min. The change in the color of the solution and the CV curves were similar. Thus, the double electrochemical switching of MVCA-C_5^{8+} to a mixture of the monomer and π-dimer tetra(radical cation) and back was also performed in the presence of Fc. This was visualized as the reversible switching of the color of the solution from yellow to blue and then to violet both in the presence and absence of the mediator. In the presence of Fc, the reverse color switching occurred much faster.

The radical products of the reduction of MVCA-C_5^{8+} and MV^{2+} were also studied by EPR. In this case, they were generated electrochemically on a Pt electrode at a controlled potential of the first reduction peak under the same conditions as during the electrolysis and CV. In 90% DMF, the spectrum of MV^{2+} was typical [58] for the $MV^{+\bullet}$ radical cation (g = 2.0030, a2N = 0.4187, a6H = 0.4017, a4H = 0.1607, a4H = 0.1319 mT). The integrated intensity of the EPR signal increased in time and the limiting value decreased proportionally when the concentration of MV^{2+} decreased fourfold (Fig. 7*a*, 7*b*). The solution was blue after the electrolysis in both cases and colored uniformly throughout the whole volume being scanned. Evidently, π-dimerization did not occur at a concentration of MV^{2+} of 2 mM and the whole amount of the generated radical cations was in the monomer form.

To model the radical cation of the methylviologen fragment of tetraviologen calix[4]resorcin, we recorded the spectrum of the methylcetylviologen radical cation (Fig. 6*c*) under the same conditions and obtained the following characteristics during spectrum simulation: g = 2.0030, aN1 = 0.4175, aN2 = 0.4018, a3H(CH_3) = 0.3989, a2H(CH_2) = 0.2614, a2H = 0.1675, a2H = 0.1503, a2H = 0.1426, and a2H = 0.1245 mT.

When MVCA-C_5^{8+} was reduced (C = 0.5 and 0.125 mM), the spectrum of the methylviologen fragment radical cation was recorded: g = 2.0030, aN1 = 0.3998, aN2 = 0.3991, a3H(CH_3) = 0.4011, a2H(CH_2) = 0.2657, a2H = 0.1765, a2H = 0.1723, a2H = 0.1361, and a2H = 0.1320 mT (Fig. 6*b*; Figs. 8*a*, 8*b*). The integrated intensity of the EPR signal increased with time to a plateau and its limiting value decreased threefold when the concentration of MVCA-C_5^{8+} decreased fourfold (Figs. 7*c*, 7*d*). The solution was violet after the electrolysis at both concentrations. A comparison of the limiting integrated intensities of the $MV^{+\bullet}$ and MVCA-$C_5^{4+\bullet}$ radical cations at the same concentration of viologen units of 2 mM including the correction coefficient for the difference in the line width led to the conclusion that the concentration of the radical cations was four times lower in the case of MVCA-$C_5^{4+\bullet}$. This means that 25% of all radical cations are in the monomer form and 75% are π-dimers.

30% Aqueous DMSO/0.1 M NaCl medium. According to previous studies [37–39], the products of the reduction of MVCA-C_5^{8+} (MVCA-$C_5^{4+\bullet}$ and

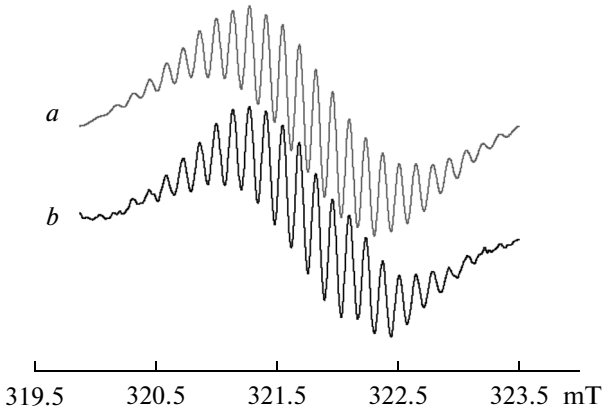

Fig. 8. (*a*) Simulated and (*b*) experimental EPR spectra of the radical cation of the methylviologen fragment generated during the electrochemical reduction at the potentials of the first peak of the reduction of MVCA-C_5^{8+} on a Pt electrode in 90% aqueous DMF/0.1 M $NaClO_4$. $C = 0.5$ mM.

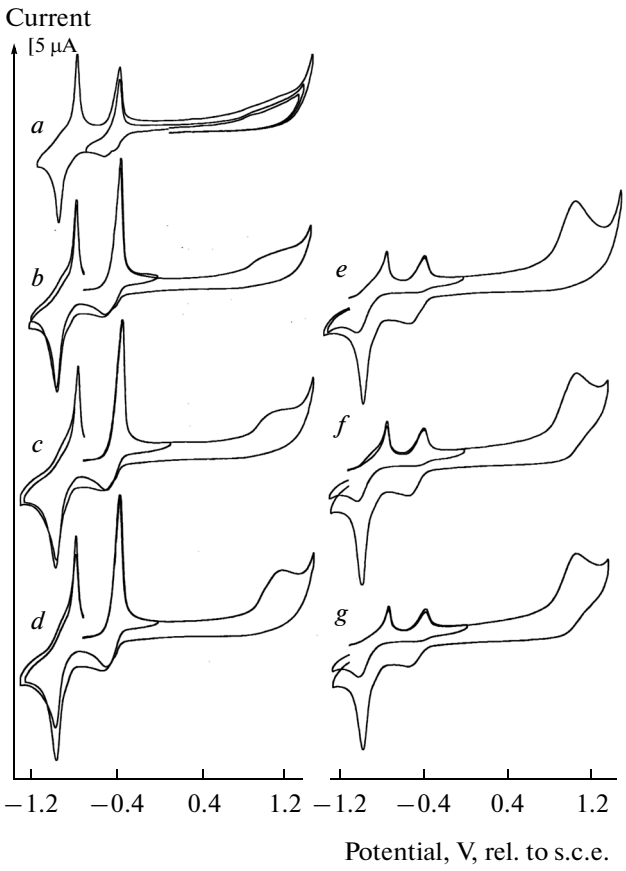

Fig. 9. CV curves of MVCA-C_5^{8+} (0.5 mM) in DMSO–H_2O (30 vol % DMF)/0.1 M NaCl: (*a*) the starting solution; (*b*)–(*d*) the solution after keeping the working electrode potential at $E = -0.7$ V for (*b*) 1, (*c*) 2, and (*d*) 3 min; (*e*)–(*g*) the solution after keeping the working electrode potential at $E = -1.1$ V for (*e*) 1, (*f*) 2, and (*g*) 3 min. v = 100 mV/s.

MVCA-C_5^0) in this medium are adsorbed on the surface of the GC electrode. The starting octacation is also partially adsorbed. The obtained CV curve (Fig. 9) agrees with these conclusions. After the electrode was maintained at the potential of MVCA-$C_5^{4+\bullet}$ generation ($E = -0.7$ V) for 1 min, the height of the acute adsorption peak of monomer oxidation ($E_{p,ox} = -0.35$ V) increased approximately threefold. The anode region acquires an extended irreversible oxidation peak ($E_p \sim 1.00$ V), which was absent on the CV curve without accumulation (Fig. 9). When the storage time increased to 2 and 3 min, the shape and height of the adsorption peak of oxidation of the MVCA-$C_5^{4+\bullet}$ monomer did not change; the additional anode peak increased and shifted toward higher positive potentials (Table 1). The cathode region contains the usual two peaks of the reduction of MVCA-C_5^{8+} (Fig. 9). Consequently, in the medium containing a larger amount of water (70%), the generated monomeric MVCA-$C_5^{4+\bullet}$ are adsorbed on the electrode in a small limiting amount. They are united into associates $(\text{MVCA-}C_5^{4+\bullet})_n$, which are much more difficult to oxidize. The number and/or size of associates increases with the electroreduction time and the difficulty of oxidation increases. After the electrolysis for 1 min or more, the associates are accumulated near the electrode and on its surface, but are not adsorbed and do not hinder the reduction of MVCA-C_5^{8+}.

In large-scale electrolysis with the solution stirred at the potentials of the first reduction peak ($E = -0.7$ V), the solution became violet throughout its volume within 1 min without intermediate blue coloring. During the electrolysis (41 min), the color of the solution became deeper, while the solution remained homogeneous. The associates did not accumulate in the near-electrode layer any longer in this case, but were uniformly distributed in the solution due to convection. After the electrolysis, the indicator microelectrode took the potential $E_{st} = -0.20$ V, which is much higher positive than the oxidation potential of the monomeric tetra(radical cation) ($E_{p,ox} = -0.38$ V). This is possible only in the case when the solution does not contain this monomer form. On the CV curve of the electrolysate in the cathode region, both peaks of the reduction of MVCA-C_5^{8+} are reduced threefold and the anode region has no oxidation peaks (Fig. 10). It follows from these data that (1) 66% MVCA-C_5^{8+} was reduced to MVCA-$C_5^{4+\bullet}$ during the electrolysis; (2) the MVCA-$C_5^{4+\bullet}$ monomer particles are recorded only on the surface of the generating electrode in the adsorbed form, but are almost absent in solution and are all united into the associate, in which the radical cations of the methylviologen fragments are largely π-dimerized; (3) this

Table 1. Potentials (V) and currents (μA) of the reduction and reoxidation peaks of MVCA-C_5^{8+} ($C = 0.5$ mM) obtained by CV on a GC electrode in DMSO–H_2O (30 vol % DMSO)/0.1 M NaCl after keeping the electrode at $E = -0.70$ V and $E = -1.10$ V for different periods of time; $v = 100$ mV/s

Electrode holding potential E, V	Holding time, min	MVCA-C_5^{8+}								
		$E^1_{p,red}$	$\Sigma I^1_{p,red}$	$E^1_{p,reox}$	$I^1_{p,reox}$	$E^2_{p,red}$	$I^2_{p,red}$	$E^2_{p,reox}$	$I^2_{p,reox}$	$E_{p,ox}$ (~I_p)
–	–	−0.51(−0.39)	10.0	−0.35	21.5	−0.95	30.0	−0.75	34.5	–
−0.7	1	−0.51(−0.40)	10.0	−0.37	59.0	−0.95	34.0	−0.78	40.5	0.98 (~2.5)
		−0.49	12.0	−0.37	59.0	−0.95	35.5	−0.78	43.5	–
	2	−0.51(−0.40)	11.5	−0.33	63.5	−0.96	34.5	−0.75	45.0	1.10 (~5)
		−0.48	15.0	−0.33	63.5	−0.98	34.5	−0.75	45.0	–
	3	−0.51(0.40)	13.0	−0.35	64.0	−0.97	41.0	−0.77	49.0	1.15 (~10)
		−0.48	15.5	−0.35	64.0	−0.97	30.0	−0.77	40.0	–
−1.1	1	−0.53	11.5	−0.38	10.5	−0.97	36.5	−0.74	15.5	1.05
		–	–	−0.38	10.5	−1.02	9.0	−0.74	15.5	–
	2	−0.53	10.5	−0.38	11.0	−0.98	39.0	−0.74	16.5	1.06
		–	–	−0.38	11.0	−1.02	9.0	−0.74	16.5	–
	3	−0.53	8.5	−0.37	9.0	−1.01	35.0	−0.73	13.5	1.06
		–	–	−0.37	9.0	−1.01	9.0	−0.73	13.5	–

associate does not settle on the electrode and goes into solution on stirring; and (4) the associate is not oxidized under the conditions of CV in the accessible range of potentials.

Under the conditions of large-scale electrolysis, the associate is completely oxidized into the starting MVCA-C_5^{8+} even at low anode potentials. Thus, during the reverse oxidation of the preceding solution at $E = +0.4$ V for 80 min, the solution completely returns to the starting state according to its color and CV curves. During the recording of the CV curves, the solution is not stirred and the substances move to the electrode surface only due to self-diffusion. Therefore, the absence of oxidation peaks on the CV curve of the reduction product may be due to the inability of the associate to be oxidized at the potentials in question or to the low rate of its self-diffusion because of its high molecular mass. In the first variant, the associate is oxidized via the oxidation of the MVCA-$C_5^{4+\bullet}$ monomer. Though its equilibrium concentration in solution is very low, the associate slowly dissociates during its oxidation and is quantitatively oxidized via the monomer form to the starting octacation during prolonged electrolysis. In the second variant, the associate itself is oxidized; during the electrolysis, the solution is stirred and convective diffusion accelerates the oxidation.

To understand the nature of not readily oxidizable species, we studied the reduction of MVCA-C_5^{8+} in the presence of a mediator, which was the anion form of ferrocenylphosphinic acid Fc-P(O)(H)OH soluble in this medium. The deprotonated form of phosphinic acid Fc-P(O)(H)O^- (**Fc-H_1**) was prepared by introducing a threefold amount of alkali (NaOH, C = 1.5 mM) in the solution. The CV curve of the Fc-H_1 anion ($C = 0.5$ mM) shows the reversible single-electron diffusion-controlled oxidation peak at $E_{p,ox} = +0.3$ V. When an equimolar amount of MVCA-C_5^{8+} was added to this solution, all the peaks of the reduction and reoxidation of MVCA-C_5^{8+} and oxidation and re-reduction of Fc-H_1 corresponded, in all parameters, to the free states of the particles (Fig. 11, Table 2).

In the preliminary reduction of the MVCA-C_5^{8+} octacation to the tetra(radical cation) state MVCA-$C_5^{4+\bullet}$ ($E = -0.7$ V) for 2 min, the adsorption peak of reoxidation of MVCA-$C_5^{4+\bullet}$ increased 1.9-fold and the oxidation current of Fc-H_1 ($E_{p,ox} = +0.37$ V) increased fourfold. The reverse peak of re-reduction of Fc-H_1^+ remained of the same height as that for Fc-H_1 in the starting solution (Table 2, Fig. 12). In addition, the reoxidation peak at 1.0 V, which was observed in the absence of Fc-H_1, disappeared on the CV curve. An increase in the reduction time to 4 and 6 min led to noticeable changes in the characteristics of only the oxidation peak of Fc-H_1 (a significant increase in its height and the broadening and shift to the anodic regions of potentials). The obtained results show that

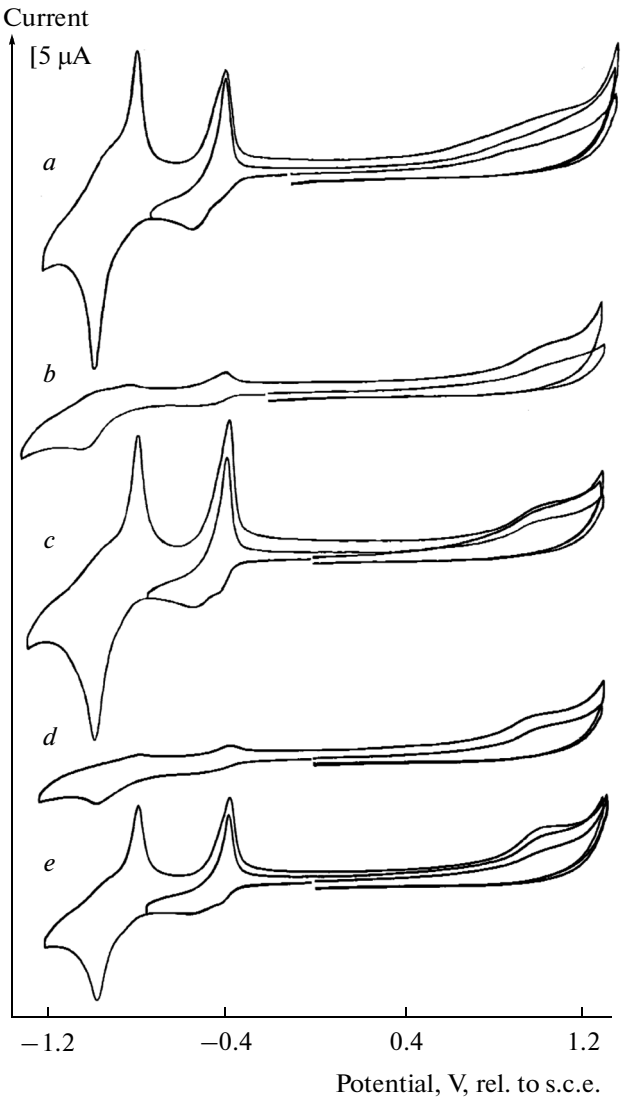

Fig. 10. CV curves of MVCA-C_5^{8+} (0.5 mM) in DMSO–H_2O (30 vol % DMF)/0.1 M NaCl: (*a*) the starting solution; (*b*) the solution after the reduction at $E = -0.7$ V and (*c*) reoxidation at $E = 0.4$ V; (*d*) the solution after the reduction at $E = -1.1$ V and (*e*) reoxidation at $E = 0.4$ V. $v = 100$ mV/s.

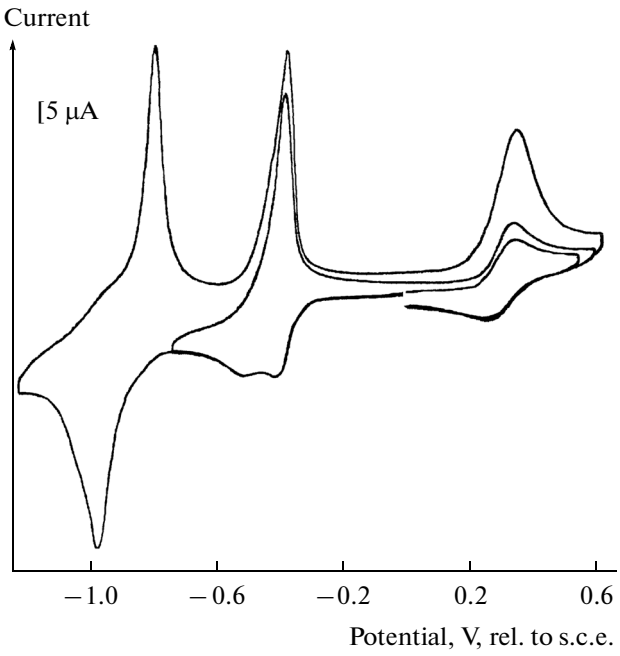

Fig. 11. Cyclic voltammogram for the MVCA-C_5^{8+} (0.5 mM)–Fc-H_1 (0.5 mM) + NaOH (1.5 mM) system recorded on a GC electrode in H_2O–DMSO (30 vol % DMSO)/0.1 M NaCl. $v = 100$ mV/s.

(1) the starting MVCA-C_5^{8+} and the products of its reduction do not bind the Fc-H_1 anion at the first stage; (2) at the Fc-H_1 oxidation potentials, the mediator oxidation of $(\text{MVCA-}C_5^{4+\bullet})_n$ associates occurs; the associates are directly oxidized on the electrode at $E_p \geq +1.0$ V; and (3) the increase in the reduction time leads to their accumulation in the near-electrode zone. If these particles are not oxidized, the height and potential of the first peak of MVCA-C_5^{8+} reduction are independent of their accumulation time and correspond to the starting free MVCA-C_5^{8+} (Fig. 12). In other words, the accumulation of $(\text{MVCA-}C_5^{4+\bullet})_n$ particles in the near-electrode zone does not affect the diffusion or reduction of MVCA-C_5^{8+}, i.e., the particles are not adsorbed or deposited on the electrode surface. If the $(\text{MVCA-}C_5^{4+\bullet})_n$ particles are oxidized via a mediator, the MVCA-C_5^{8+} reduction current increases in direct proportion to the amount of the accumulated product. Consequently, the mediator oxidation of $(\text{MVCA-}C_5^{4+\bullet})_n$ again leads to the formation of MVCA-C_5^{8+}.

To estimate the rate of dissociation and diffusion of the $(\text{MVCA-}C_5^{4+\bullet})_n$ associate, we performed another series of experiments. After the working electrode was kept at the first reduction peak potential (−0.70 V) for 2 min, the CV curve was recorded with an initial scan in the anodic region. The scanning was stopped at a potential of −0.15 V and this potential was maintained each time for different periods of time (10 to 500 s). At this potential, the MVCA-$C_5^{4+\bullet}$ monomer was oxidized, but high-molecular $(\text{MVCA-}C_5^{4+\bullet})_n$ was not. The dissociation of $(\text{MVCA-}C_5^{4+\bullet})_n$ into monomer species is fast enough, but $(\text{MVCA-}C_5^{4+\bullet})_n$ can also be quickly oxidized to the starting MVCA-C_5^{8+} at this potential. As the storage time at a potential of −0.15 V increased, the oxidation peak of substituted ferrocene decreased. The intensity of this peak also significantly decreased when the potential was switched off for 10 min after it reached −0.15 V. However, the height of

Table 2. Potentials (V) and currents (μA) of the reduction and reoxidation peaks of MVCA-C_5^{8+} ($C = 0.5$ mM) and of the oxidation of Fc-H_1 ($C = 0.5$ mM) in a mixture obtained by CV on a GC electrode in DMSO–H_2O (30 vol % DMSO)/0.1 M NaCl in the presence of NaOH (1.5 mM) after holding the working electrode potential at $E = -0.70$ V and $E = -1.10$ V for different periods of time; $v = 100$ mV/s

Electrode holding potential, V	Holding time, min	MVCA-C_5^{8+}								Fc-H_1	
		$E^1_{p,red}$	$\Sigma I^1_{p,red}$	$E^1_{p,reox}$	$I^1_{p,reox}$	$E^2_{p,red}$	$I^2_{p,red}$	$E^2_{p,reox}$	$I^2_{p,reox}$	$E_{p,ox}$	$E_{p,rered}$
–	–	–0.49 (0.40)	12	–0.37	30	–0.97	27.5	–0.77	37.5	0.34	0.26
–0.70	1	–0.45	15	–0.35	57	–0.97	41.0	–0.78	44.0	–	–
		–0.48	17	–0.35	57	–0.97	44.0	–0.78	49.0	0.37	0.26
	2	–0.48	18	–0.34	65	–0.99	46.0	–0.77	51.0	–	–
		–0.48	24	–0.34	65	–0.98	64.0	–0.77	61.0	0.39	0.27
	3	–0.48	17	–0.34	66	–0.99	44.0	–0.77	46.0	–	–
		–0.48	27	–0.34	66	–0.99	69.0	–0.77	63.0	0.42	0.27
	4	–0.48	15	–0.34	68	–1.00	36.0	–0.77	42.0	–	–
		–0.48	35	–0.34	68	–0.99	88.0	–0.77	74.0	0.41	0.27
	5	–0.47	15	–0.34	68	–1.03	30.0	–0.77	45.0	–	–
		–0.48	36	–0.34	68	–0.99	91.0	–0.77	72.0	0.43	0.26
	6	–0.47	16	–0.34	70	–1.00	35.0	–0.77	40.0	–	–
		–0.47	40	–0.34	70	–0.99	95.0	–0.77	78.0	0.44	0.26
–1.10	1	–1.06	21	–0.38	14	–	–	–0.75	14.0	–	–
		–0.49	18	–0.38	18	–0.97	49.0	–0.75	14.0	0.37	0.26
	2	–1.06	22	–0.38	17	–	–	–0.75	12.0	–	–
		–0.49	23	–0.38	17	–0.98	63.0	–0.75	12.0	0.42	0.26
	3	–1.06	25	–0.38	14	–	–	–0.75	15.0	–	–
		–0.49	26	–0.38	17	–0.98	74.0	–0.75	15.0	0.42	–
	4	–1.06	31	–0.37	18	–	–	–0.74	15.0	–	–
		–0.48	29	–0.37	18	–0.98	81.0	–0.74	15.0	0.43	–
	5	–1.06	28	–0.38	16	–	–	–0.74	12.0	–	–
		–0.49	32	–0.38	19	–0.99	82.0	–0.74	15.0	0.39	–
	6	–1.06	28	–0.38	18	–	–	–0.74	15.0	–	–
		–0.48	32	–0.38	20	–0.98	84.0	–0.74	16.0	0.41	–

the oxidation peak under study was higher than that of the corresponding peak of individual Fc-H_1 in all cases. Evidently, the $(MVCA\text{-}C_5^{4+\bullet})_n$ associate has high molecular weight, slowly dissociates into monomeric MVCA-$C_5^{4+\bullet}$, and has such a low diffusion coefficient that even 10 min is not enough for it to completely diffuse from the electrode surface to the solution.

In large-scale electroreduction (–0.7 V, 120 min) and reverse oxidation (+0.5 V, 10 min) in the presence of Fc-H_1, the cycle of transformations was the same as in the absence of a mediator. 70% MVCA-C_5^{8+} transformed into the soluble $(MVCA\text{-}C_5^{4+\bullet})_n$ associate (the yellow solution turned violet) during the reduction and completely returned to the starting yellow substance during the reverse oxidation. In the presence of a mediator, however, the oxidation was eight times faster. Another difference was a slight decrease in the intensity of the violet coloring after a certain value was reached. Fc-H_1 was included in the high-molecular associate, as indicated by the decreased oxidation peak after the reduction stage (Fig. 13). The repeated reduction– reoxidation cycle led to the same results.

The radical products of the reduction of MVCA-C_5^{8+} and MV^{2+} were studied in this medium by EPR using the same algorithm as in 90% DMF. The results

were similar. The spectra of the methylviologen radical cations and methylviologen fragments of calixresorcin were recorded. The signal intensity increased with the electrolysis time to the limiting value (Fig. 14). When the concentration of the substance increased fourfold, the limiting integrated intensity changed fourfold (MV^{2+}) and 3.5-fold (MVCA-C_5^{8+}). The color of the solution after the electrolysis was blue for MV^{2+} and violet for MVCA-C_5^{8+}. However, there were appreciable differences. Despite prolonged electrolysis for 60 min, the violet coloring was concentrated in the near-electrode area and the intensity of the EPR signal for MVCA-$C_5^{4+\bullet}$ was 10 times lower than for $MV^{+\bullet}$. According to EPR, in 30% DMSO, π-dimerization was higher; 90% radical cations of the viologen fragments were in the form of the π-dimer; and the π-dimer particles were in the high-molecular product, which did not markedly diffuse from the near-electrode zone in the solution within at least 1 h.

Thus, the association of tetraviologen calix[4]resorcin MVCA-C_5^{8+} can be controlled using the electrochemical cycle of the reduction–reoxidation of its viologen units in 30% aqueous DMSO. The reduction of the MVCA-C_5^{8+} monomer to the MVCA-$C_5^{4+\bullet}$ tetra(radical cation) leads to its transformation into the high-molecular associate (π-polymer) (MVCA-$C_5^{4+\bullet}$)$_n$, its reverse oxidation fully returned it to its original monomer state (Scheme 3). In this medium, the color switched from yellow to violet and back.

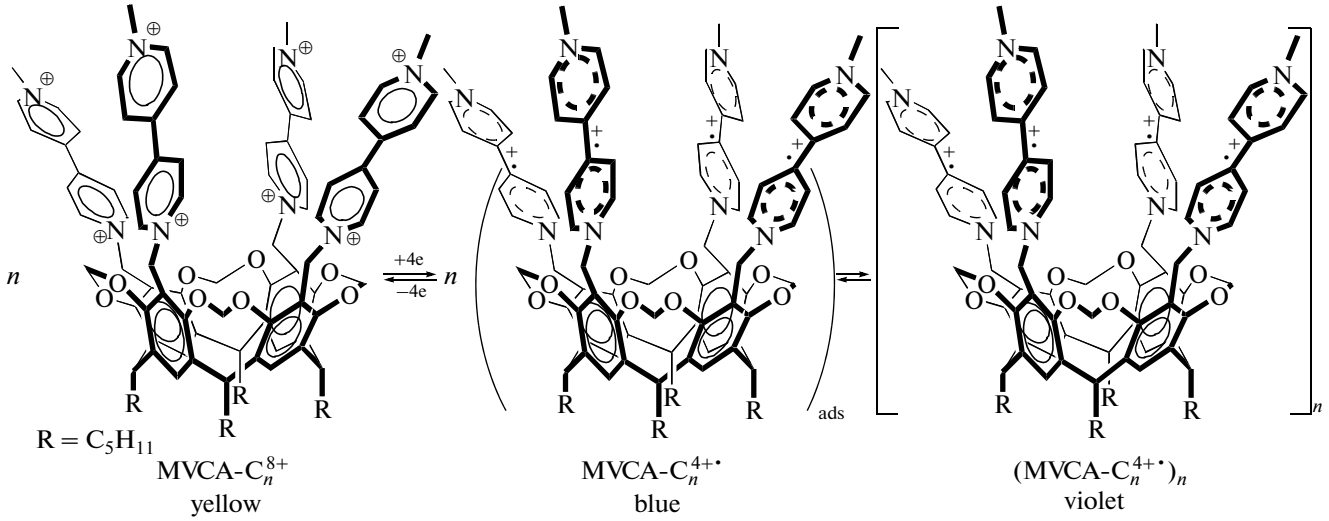

Scheme 3. Reversible electroswitching of the MVCA-C_5^{8+} monomer to the high-molecular associate (π-polymer) (MVCA-$C_5^{4+\bullet}$)$_n$.

Then we also studied the system by CV and electrolysis under the conditions of the reduction of MVCA-C_5^{8+} to MVCA-C_5^0. When the electrode was preliminarily kept at the potentials of the second stage of the reduction of MVCA-C_5^{8+} ($E = -1.10$ V), the CV curve acquired an irreversible oxidation peak at 1.06 V in addition to the two usual adsorption peaks of oxidation of the reduction products; the height of this additional peak was practically independent of the accumulation time (1, 2, and 3 min). Obviously, as in the case of MVCA-$C_5^{4+\bullet}$, the completely reduced MVCA-C_5^0 form is adsorbed on the electrode and forms the associates that are oxidized at $E_p = 1.06$ V (Table 1). After the oxidation of the associates, the reverse branch of CV contains two normal reduction peaks of MVCA-C_5^{8+} (Fig. 9). If the associates are not oxidized, the reverse branch contains only one reduction peak (at $E_p = -1.02$ V) instead of two peaks in the accessible range of potentials. The potential of this peak is higher negative than that of both reduction peaks of MVCA-C_5^{8+} under the normal conditions; the peak current is independent of the generation time of the MVCA-C_5^0 neutral form and is comparable to the current of the first stage of the reduction of MVCA-C_5^{8+} in the starting solution. All this is caused by the fact that (MVCA-C_5^0)$_n$ is deposited on the electrode surface and hinders the supply of MVCA-C_5^{8+} to the electrode surface and its reduction at the first stage (~0.50 V), but affects little, if at all, the second stage potential. Therefore, both stages of reduction are performed at the same potential.

The reduction–reoxidation cycle was also performed under the large-scale electrolysis conditions. The reduction was conducted at −1.1 V for 120 min.

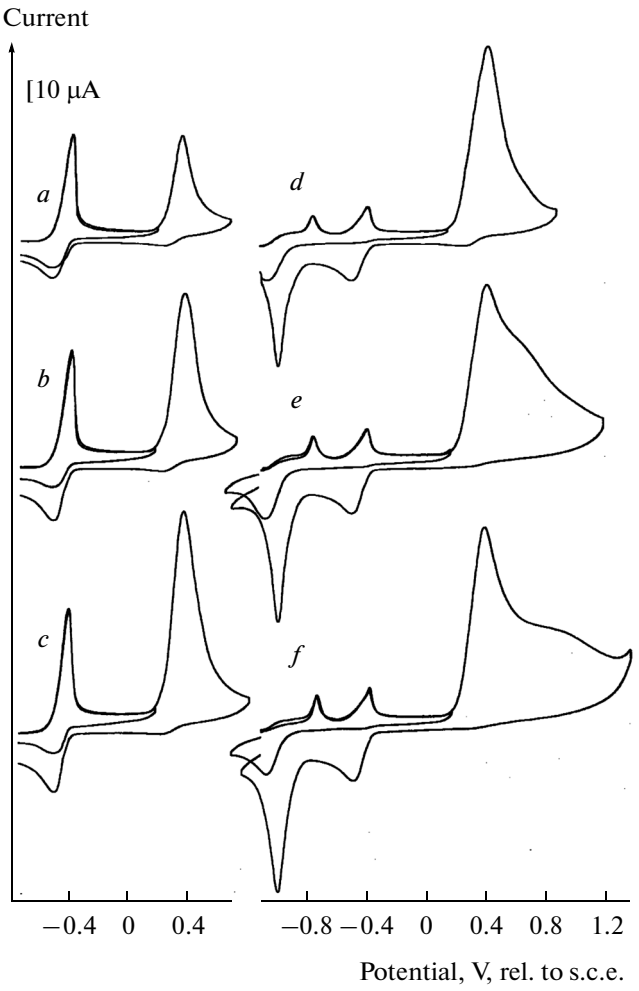

Fig. 12. CV curves of the MVCA-C_5^{8+} (0.5 mM)–Fc-H_1 (0.5 mM) + NaOH (1.5 mM) system recorded on a GC electrode in H_2O–DMSO (30 vol % DMSO)/0.1 M NaCl after the working electrode potential was kept at E = −0.7 V for (*a*) 2, (*b*) 4, and (*c*) 6 min and at E = −1.1 V for (*d*) 2, (*e*) 4, and (*f*) 6 min. v = 100 mV/s.

The solution was homogeneous and colorless, then became light-violet, and again almost colorless. After the reduction, the solution contained 15% of the starting MVCA-C_5^{8+} (CV, Fig. 10), but no MVCA-C_5^0 and MVCA-$C_5^{4+\bullet}$ monomers. This is indicated by the steady-state potential of the indicator GC electrode (E_{st} = 0.04 V). Despite the stirring of the solution during the electrolysis, the whole amount of the $(MVCA\text{-}C_5^0)_n$ associate obviously deposited on the surface of the generating electrode (GC fabric). According to CV data, the starting compound is recovered during the reverse oxidation at +0.4 V. In the electrooxidation, the oxidized currents decrease, reaching the minimum value after 150 min. In this case, only 70% of the starting compound is regenerated; the other 30% are completely recovered during the after-oxidation with atmospheric oxygen.

The generation of neutral MVCA-C_5^0 was also studied in the presence of the electrochemically generated Fc-H_1^+ mediator. After 2-min storage of the electrode at E = −1.10 V, the heights of the two adsorption peaks of oxidation of MVCA-C_5^0 decreased approximately 3.5-fold and the oxidation peak of Fc-H_1 increased significantly (Fig. 12). The increase in the storage time did not affect the adsorption peaks, but led to an increase in the height and width of the oxidation peak of Fc-H_1. In this case again, the hardly oxidizable $(MVCA\text{-}C_5^0)_n$ particles were evidently easily oxidized via a mediator with the electrochemically generated Fc-H_1^+. Unlike $(MVCA\text{-}C_5^{4+\bullet})_n$, these particles are deposited on the electrode surface and hinder the supply of the substance to the electrode surface and the electrochemical reactions. That is why the adsorption maxima of oxidation of MVCA-C_5^0 decreased and the first reduction peak of MVCA-C_5^{8+} shifted 0.57 V toward higher negative potentials. In the mediator (Fc-H_1) oxidation of these particles, the curve contains the reduction peaks of MVCA-C_5^{8+} at the same potentials as for the starting calixresorcin, but with increased heights. These heights increase with the exposure time. This means that the mediator oxidation again forms the starting compound.

The reduction–reoxidation cycle in the presence of Fc-H_1 in large-scale electrolysis proceeded in the same way as in the absence of a mediator. The reduction (−1.1 V, 120 min) of 90% MVCA-C_5^{8+} formed the colorless high-molecular associate $(MVCA\text{-}C_5^0)_n$, as the sole product, which fully deposited on the electrode surface. This associate did not include the mediator. The whole amount of Fc-H_1 was in solution and its electrochemical characteristics fully corresponded to those of the initial state. The reverse mediator oxidation (+0.5 V, 10 min) followed by after-oxidation with air oxygen completely returned the compound to its starting state MVCA-C_5^{8+}.

Thus, MVCA-C_5^{8+} was transferred from solution to the deposit and then back into solution during the cycle of reduction (at the second stage potentials) – reoxidation (+(0.4–0.5) V) both in the absence and presence of a mediator.

CONCLUSIONS

The electrochemical reduction of tetraviologen calix[4]resorcin MVCA-C_5^{8+} in organic (DMF, DMSO), aqueous organic, and aqueous solutions involved the two-stage reduction of viologen fragments to the radical cation and neutral diamine. All viologen units were reduced at the same potential; the overall process

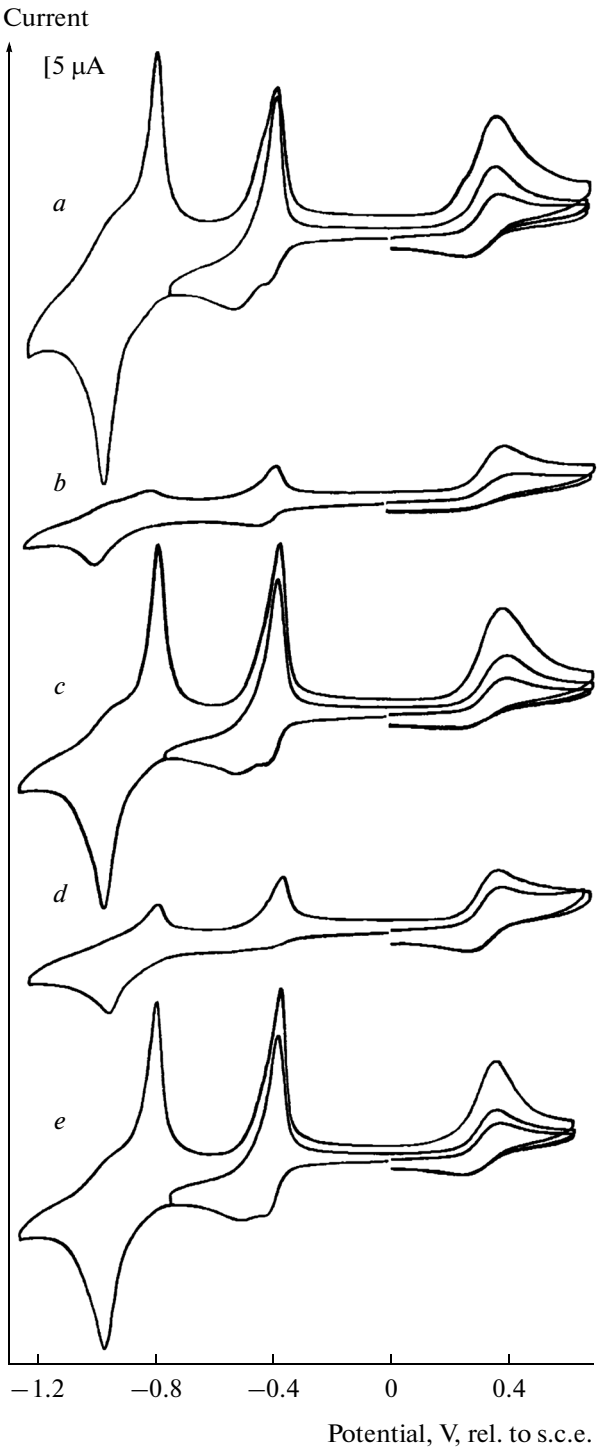

Fig. 13. CV curves of the MVCA-C_5^{8+} (0.5 mM)–Fc-H_1 (0.5 mM) + NaOH (1.5 mM) system recorded on a GC electrode in H_2O–DMSO (30 vol % DMSO)/0.1 M NaCl: (*a*) the starting solution; the solution after (*b*) the reduction at $E = -0.7$ V and (*c*) reoxidation at $E = 0.5$ V; the solution after (*d*) the reduction at $E = -1.1$ V and (*e*) reoxidation at $E = 0.5$ V. $v = 100$ mV/s.

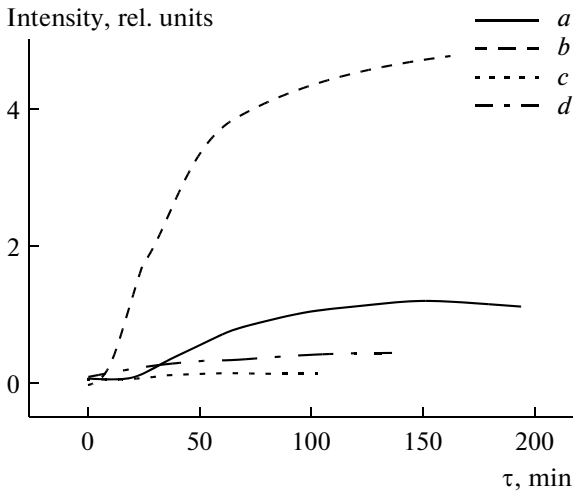

Fig. 14. Dependence of the EPR signal intensity of radical species in DMSO–H_2O (30 vol % DMF)/0.1 M $NaClO_4$ for (*a*) $MV^{+\bullet}$ ($C = 0.5$ mM), (*b*) $MV^{+\bullet}$ ($C = 2$ mM), (*c*) MVCA-$C_5^{4+\bullet}$ ($C = 0.125$ mM), and (*d*) MVCA-$C_5^{4+\bullet}$ ($C = 0.5$ mM).

occurred in two stages, forming the MVCA-$C_5^{4+\bullet}$ radical cation at the first stage and the neutral compound MVCA-C_5^0 at the second. At concentrations of MVCA-$C_5^{4+\bullet}$ of 0.02–0.04 mM in organic solvents, the radical cations of the viologen fragments existed as monomers; in aqueous organic solvents, they underwent intermolecular π-dimerization. The fraction of the π-dimer increased with the water content and the monomer was found in minor quantities in pure water. At a concentration of MVCA-$C_5^{4+\bullet}$ of 0.5 mM, the π-dimer content was 75% in 90% DMF and 90% in 30% DMSO. The methylviologen $MV^{+\bullet}$ radical cations did not dimerize under similar conditions and concentrations.

The coloring of the solution was controlled using the difference in the coloring between the starting MVCA-C_5^{8+} (yellow), the Fc, Fc-H_1 mediator (yellow), the methylviologen fragment radical cation (blue), and its π-dimer (violet), the dependence of π-dimerization on the concentration and solvent, and the reversible electrochemical cycle of first-stage reduction and the reverse mediator or mediator-free oxidation. The color switching was performed from yellow to blue and from blue to violet in 90% DMF and from yellow to violet in 30% DMSO. Similar color switchings can also be performed for ordinary viologens, but this requires higher concentrations and charges.

In 30% aqueous DMSO, the monomeric MVCA-$C_5^{4+\bullet}$ tetra(radical cations) existed only in the adsorbed form on the surface of the generating electrode. In solution they self-associated into a soluble high-molecular product. Not all radical cations were

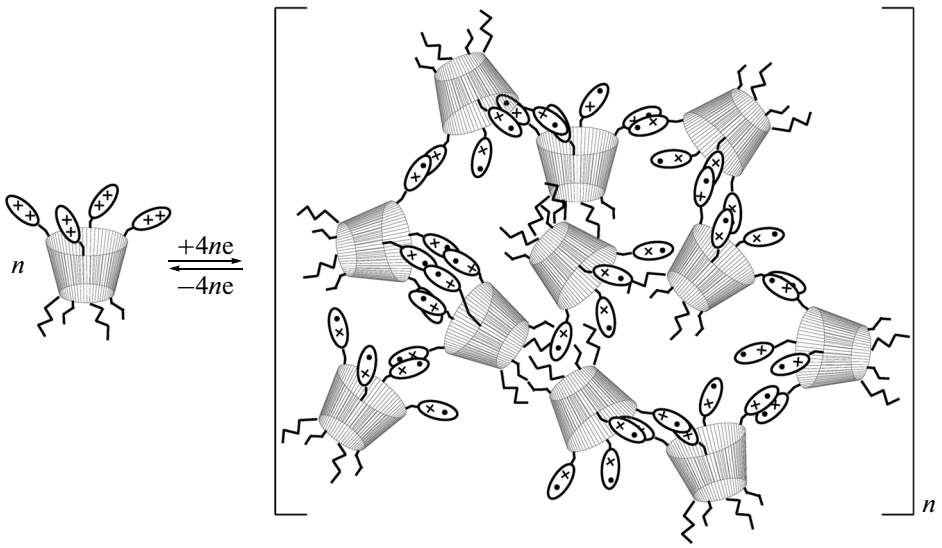

Fig. 15. Reversible electrochemical switching monomer–associate (π-polymer).

π-dimerized in the associate, 10% was in the monomer form. In the presence of the Fc-H_1 mediator, the associate also included the mediator.

The neutral compound MVCA-C_5^0 was completely hydrophobic. Therefore in 30% aqueous DMSO it formed an insoluble high-molecular associate. The generation of MVCA-C_5^0 in the presence of Fc-H_1 gave the same associate without a mediator. The associate deposited on the electrode. This deposit has good adhesion to the glassy carbon surface, does not pass in solution on stirring, and hinders both the diffusion and the electrochemical reduction of MVCA-C_5^{8+} itself.

Based on the electrochemical reduction–reoxidation cycles of viologen units, we performed electrochemical control over the association and deposition of tetraviologen calix[4]resorcin MVCA-C_5^{8+} in 30% DMSO. The reduction to the MVCA-$C_5^{4+\bullet}$ tetra(radical cation) converted the MVCA-C_5^{8+} monomer into the high-molecular associate (π-polymer) (MVCA-$C_5^{4+\bullet}$)$_n$ and its reverse oxidation completely returned it to the initial monomer state (Fig. 15). Calixresorcin was transferred from solution to deposit by the reduction to the neutral state MVCA-C_5^0 and back to solution by the reverse oxidation.

The complete return of MVCA-C_5^{8+} to the initial state after the first- or second-stage reduction cycle and reverse oxidation suggests the complete chemical reversibility of the reduction and the formation of stable high-molecular (MVCA-$C_5^{4+\bullet}$)$_n$ and (MVCA-C_5^0)$_n$ due to the noncovalent intermolecular interactions. In the case of MVCA-$C_5^{4+\bullet}$, one of such interactions is intermolecular π-dimerization with one to four interaction centers. Another reason for association is the interaction of hydrophobic calixresorcin platforms, which are not readily solvated in this aqueous organic medium. This interaction is proven by the precipitation of the neutral (MVCA-C_5^0)$_n$. These interactions are unidirectional and directed toward association; that is why the associate is high-molecular. The Fc-H_1 mediator is charged negatively, contains a hydrophobic ferrocene fragment, and is included in the associate as a counterion.

ACKNOWLEDGMENTS

This study was financially supported by the Russian Foundation for Basic Research and Tatarstan (grant nos. 12-03-00379 and 13-03-97061).

REFERENCES

1. Weitz, E., *Angew. Chem.*, 1954, vol. 66, p. 658.
2. Anelli, P.L., Ashton, P.R., Ballardini, R., Balzani, V., Delgaro, M., Gandolfi, M.T., Goodnow, T.T., Kaifer, A.E., Philp, D., Pietraszkiewicz, M., Prodi, L., Reddington, M.V., Slawin, A.M.Z., Spencer, N., Stoddart, J.F., Vincent, C., and Williams, D.J., *J. Am. Chem. Soc.*, 1992, vol. 114, p. 193.
3. Ashton, P.R., Ballardini, R., Balzani, V., Credi, A., Gandolfi, M.T., Menzer, S., Perez-Garcia, L., Prodi, L., Stoddart, J.F., Venturi, M., White, A.J.P., and Williams, D.J., *J. Am. Chem. Soc.*, 1995, vol. 117, p. 11171.
4. Ballardini, R., Balzani, V., Credi, A., Braun, C.L., Gillard, R.E., Montalti, M., Philp, D., Soddart, J.F., Venturi, M., White, A.J.P., Williams, B.J., and Williams, D.J., *J. Am. Chem. Soc.*, 1997, vol. 119, p. 12503.
5. Ashton, P.R., Balzani, V., Credi, A., Kocian, O., Pasini, D., Prodi, L., Spencer, N., Stoddart, J.F., Tol-

ley, M.S., Venturi, M., White, A.J.P., and Williams, D.J., *Chem. – Eur. J.*, 1998, vol. 4, p. 590.

6. Amabilino, D.B., Ashton, P.R., Balzani, V., Boyd, S.E., Credi, A., Lee, J.U., Menzer, S., Stoddart, J.F., Venturi, M., and Williams, D.J., *J. Am. Chem. Soc.*, 1998, vol. 120, p. 4295.
7. Balzani, V., Credi, A., Langford, S.J., Raymo, F.M., Stoddart, J.F., and Venturi, M., *J. Am. Chem. Soc.*, 2000, vol. 122, p. 3542.
8. Asakawa, M., Ashton, P.R., Balzani, V., Credi, A., Hamers, C., Mattersteig, G., Montalti, M., Shipway, A.N., Spencer, N., Stoddart, J.F., Tolley, M.S., Venturi, M., White, A.J.P., and Williams, D.J., *Angew. Chem.*, 1998, vol. 110, p. 357.
9. Balzani, V., Credi, A., Mattersteig, G., Matthews, O.A., Raymo, F.M., Stoddart, J.F., Venturi, M., White, A.J.P., and Williams, D.J., *J. Org. Chem.*, 2000, vol. 65, p. 1924.
10. Deng, W.-Q., Flood, A.H., Stoddart, J.F., and Goddart, W.A., *J. Am. Chem. Soc.*, 2005, vol. 127, p. 15994.
11. Ballardini, R., Balzani, V., Clemente-Leon, M., Credi, A., Gandolfi, M.T., Ishow, E., Perkins, J., Stoddart, J.F., Tseng, H.-R., and Wenger, S., *J. Am. Chem. Soc.*, 2002, vol. 124, p. 12786.
12. Chen, Y., Jung, G.-Y., Ohlberg, D.A.A., Li, X., Stewart, D.R., Jeppesen, J.O., Nielsen, K.A., Stoddart, J.F., and Williams, R.S., *Nanotechnology*, 2003, vol. 14, p. 462.
13. Bryce, M.R., Cooke, G., Duclairoir, F.M.A., John, P., Peperichka, D.F., Polwart, N., Rotello, V.M., Stoddart, J.F., and Tseng, H.-R., *J. Mater. Chem.,* 2003, vol. 13, p. 2111.
14. Venturi, M., Dumas, S., Balzani, V., Cao, J., and Stoddart, J.F., *New J. Chem.*, 2004, vol. 28, p. 1032.
15. Huang, T.J., Tseng, H.-R., Sha, L., Lu, W., Brough, B., Flood, A.H., Yu, B.-D., Celestre, P.C., Chang, J.P., Stoddart, J.F., and Ho, C.-M., *Nano Lett.*, 2004, vol. 4, p. 2065.
16. Liu, Y., Flood, A.H., Bonvallet, P.A., Vignon, S.A., Northrop, B.H., Tseng, H.-R., Jeppesen, J.O., Huang, T.J., Brough, B., Baller, M., Magonov, S., Solares, S.D., Goddard, W.A., Ho, C.-M., and Stoddart, J.F., *J. Am. Chem. Soc.*, 2005, vol. 127, p. 9745.
17. Nygaard, S., Laursen, B.W., Flood, A.H., Hansen, C.N., Jeppesen, J.O., and Stoddart, J.F., *Chem. Commun.*, 2006, p. 144.
18. Beckman, R., Beverly, K., Boukai, A., Bunimovich, Y., Choi, J.W., DeIonno, E., Creen, J., Johnston-Halperin, E., Luo, Y., Sheriff, B., Stoddart, J.F., and Heath, J.R., *Faraday Discuss.*, 2006, vol. 131, p. 9.
19. Diaz, M.C., Illescas, B.M., Martin, N., Stoddart, J.F., Canales, M.A., Jimenez-Barbero, J., Sarova, G., and Guldi, D.M., *Tetrahedron,* 2006, vol. 62, p. 1998.
20. Badjic, J.D., Ronconi, C.M., Stoddart, J.F., Balzani, V., Silvi, S., and Credi, A., *J. Am. Chem. Soc.*, 2006, vol. 128, p. 1489.
21. Ikeda, T., Saha, S., Aprahamian, I., Leung, K.C.-F., Williams, A., Deng, W.-Q., Flood, A.H., Goddard, W.A., and Stoddart, J.F., *Chem. – Asian J.*, 2007, vol. 2, p. 76.
22. Flamigni, L., Talarico, A.M., Serroni, S., Punterieoro, F., Gunter, M.J., Johnston, M.R., and Jeynes, T.P., *Chem. Eur. J.*, 2003, vol. 9, p. 2649.
23. Gunter, M.J., *Eur. J. Org. Chem.*, 2004, p. 1655.
24. Steuerman, D.W., Peters, A.J., Tseng, H.-R., Flood, A.H., Jeppesen, J., O., Nielsen, K.A., Heath, J.R., and Stoddart, J.F., *Angew. Chem., Int. Ed. Engl.*, 2004, vol. 43, p. 6486.
25. Flood, A.H., Peters, A.J., Vignon, S.A., Steuerman, D.W., Tseng, H.-R., Kang, S., Heath, J.R., and Stoddart, J.F., *Chem. – Eur. J.*, 2004, vol. 10, p. 6558.
26. Tseng, H.-R., Wu, D., Fang, N.X., Zhang, X., and Stoddart, J.F., *ChemPhysChem*, 2004, vol. 5, p. 111.
27. Amabilino, D.B., Ashton, P.R., Balzani, V., Braun, C.L., Credi, A., Frecheu, J.M.J., Leon, J.W., Raymo, F.M., Spencer, N., Stoddart, J.F., and Venturi, M., *J. Am. Chem. Soc.*, 1996, vol. 118, p. 12012.
28. Amabilino, D.B., Asakawa, M., Ashton, P.R., Ballardini, R., Balzani, V., Belohradsky, M., Credi, A., Higuchi, M., Raymo, F.M., Shimizu, T., Stoddart, J.F., Venturi, M., and Yase, K., *New J. Chem.,* 1998, vol. 22, p. 959.
29. Bissel, R.A., Crdova, E., Kaifer, A.E., and Stoddart, J.F., *Nature*, 1994, vol. 369, p. 133.
30. Yasuda, T., Tanabe, K., Tsuji, T., Coti, K.K., Aprahamian, I., Stoddart, J.F., and Kato, T., *Chem. Commun.*, 2010, vol. 46, p. 1224.
31. Ashton, P.R., Ballardini, R., Balzani, V., Boyd, S.E., Credi, A., Gandolfi, M.T., Gomez-Lopez, M., Iqbal, S., Philp, D., Preece, J.A., Prodi, L., Ricketts, H.G., Stoddart, J.F., Tolley, M.S., Venturi, M., White, A.J.P., and Williams, D.J., *Chem. – Eur. J.*, 1997, vol. 3, p. 152.
32. Tseng, H.-R., Vignon, S.A., and Stoddart, J.F., *Angew. Chem., Int. Ed. Engl.*, 2003, vol. 42, p. 1491.
33. Liu, Y., Flood, A.H., and Stoddart, J.F., *J. Am. Chem. Soc.,* 2004, vol. 126, p. 9150.
34. Asakawa, M., Ashton, P.R., Balzani, V., Credi, A., Mattersteig, G., Matthews, O.A., Montalti, M., Spencer, N., Stoddart, J.F., and Venturi, M., *Chem. Eur. J.*, 1997, vol. 3, p. 1992.
35. Ziganshina, A.Y., Kharlamov, S.V., Korshin, D.E., Mukhitova, R.K., Kazakova, E.Kh., Latypov, Sh.K., Yanilkin, V.V., and Konovalov, A.I., *Tetrahedron Lett.*, 2008, vol. 49, p. 5312.
36. Nasybullina, G.R., Yanilkin, V.V., Nastapova, N.V., Korshin, D.E., Ziganshina, A.Y., and Konovalov, A.I., *J. Inclusion Phenom. Macrocyclic Chem.*, 2012, vol. 72, p. 299.
37. Nasybullina, G.R., Yanilkin, V.V., Nastapova, N.V., Ziganshina, A.Yu., Korshin, D.E., Spiridonova, Yu.S., Karasik, A.A., and Konovalov, A.I., *Izv. Akad. Nauk, Ser. Khim.*, 2012, p. 2274.
38. Yanilkin, V.V., Mustafina, A.R., Stepanov, A.S., Nastapova, N.V., Nasybullina, G.R., Ziganshina, A.Y., Solovieva, S.E., and Konovalov, A.I., *Russ. J. Electrochem.*, 2011, vol. 47, p. 1082.
39. Ziganshina, A.Yu., Nasybullina, G.R., Yanilkin, V.V., Nastapova, N.V., Korshin, D.E., Spiridonova, Yu.S., Kashapov, R.R., Grüner, M., Habicher, W.D., Karasik, A.A., and Konovalov, A.I., *Russ. J. Electrochem.*, 2014, vol. 50, no. 2, pp. 142–153.

40. Kosower, E.M. and Hajdu, J., *J. Am. Chem. Soc.*, 1964, vol. 93, p. 2534.

41. Kimura, K., Yamada, H., and Tsubomura, H., *J. Chem. Phys.*, 1971, vol. 48, p. 440.

42. Itoh, M. and Kosower, E.M., *J. Am. Chem. Soc.*, 1968, vol. 90, p. 1843.

43. Kosower, E.M. and Teuerstein, A., *J. Am. Chem. Soc.*, 1976, vol. 98, p. 1586.

44. Weitz, E., *Ber. Dtsch. Chem. Ges.,* 1942, vol. 79, p. 1927.

45. Evans, A.G., Evans, J.C., and Baker, M.W., *J. Chem. Soc., Perkin Trans. 2*, 1977, p. 1787.

46. Evans, A.G., Evans, J.C., and Rees, N.H., *J. Chem. Soc., Perkin Trans. 2*, 1975, p. 1831.

47. Evans, A.G., Dodson, N.K., and Rees, N.H., *J. Chem. Soc., Perkin Trans. 2*, 1976, p. 859.

48. Bird, C.L. and Kuhn, A.T., *Chem. Soc. Rev.*, 1981, vol. 10, p. 49.

49. Jeon, W.S., Ziganshina, A.Y., Lee, J.W., Ko, Y.H., Kang, J.K., Lee, C., and Kim, K., *Angew. Chem., Int. Ed. Engl.*, 2003, vol. 42, p. 4097.

50. Lee, J.W., Hwang, I., Jeon, W.S., Ko, Y.H., Sakamoto, S., Yamaguchi, K., and Kim, K., *Chem. Asian J.*, 2008, vol. 3, p. 1277.

51. Jeon, W.S., Kim, E., Ko, Y.H., Hwang, I., Lee, J.W., Kim, S.-Y., Kim, H.-J., and Kim, K., *Angew. Chem., Int. Ed. Engl.*, 2005, vol. 44, p. 87.

52. Zhu, Z., Fahrenbach, A.C., Li, H., Barnes, J.C., Liu, Z., Dyar, S.M., Zhang, H., Lei, J., Carmieli, R., Sarjeant, A.A., Stern, Ch.L., Wasielewski, M.R., and Stoddart, J.F., *J. Am. Chem. Soc.*, 2012, vol. 134, p. 11709.

53. Galus, Z., *Foundations of Electrochemical Analysis,* New York: Harwood, 1976.

54. Shekurov, R.P., Miluykov, V.A., Islamov, D.R., Krivolapov, D.B., Kataeva, O.N., Gerasimova, T.P., Katsyuba, S.A., Nasybullina, G.R., Yanilkin, V.V., and Sinyashin, O.G., *J. Organomet. Chem.*, 2014, vol. 766, p. 40.

55. Gordon, A.J. and Ford, R.A., *The Chemist's Companion*, New York: Wiley-Interscience, 1972.

56. Peinador, C., Roman, E., Abboud, Kh., and Kaifer, A.E., *Chem. Commun.*, 1999, p. 1887.

57. Roman, E., Chas, M., Quintela, J.M., Peinador, C., and Kaifer, A.E., *Tetrahedron*, 2002, vol. 58, p. 699.

58. Johnson, C.S. and Gutowsky, H.S., *J. Chem. Phys.*, 1963, vol. 39, p. 58.

Translated by L. Smolina